HHS Public Access

Author manuscript

J Mol Cell Cardiol. Author manuscript; available in PMC 2017 January 01.

Published in final edited form as:

J Mol Cell Cardiol. 2016 January ; 90: 74–83. doi:10.1016/j.yjmcc.2015.12.001.

Early Cardiac Dysfunction in the Type 1 Diabetic Heart Using Speckle-Tracking Based Strain Imaging

Danielle L. Shepherd[a], **Cody E. Nichols**[a], **Tara L. Croston**[a], **Sarah L. McLaughlin**[b], **Ashley B. Petrone**[c], **Sara E. Lewis**[a], **Dharendra Thapa**[a], **Dustin M. Long**[d], **Gregory M. Dick**[a], and **John M. Hollander**[a]

[a]Department of Exercise Physiology, Center for Cardiovascular and Respiratory Sciences, School of Medicine, West Virginia University, Morgantown, WV, 26505

[b]Department of Cancer Cell Biology, School of Medicine, West Virginia University, Morgantown, WV, 26505

[c]Department of Neurobiology and Anatomy, School of Medicine, West Virginia University, Morgantown, WV, 26505

[d]Department of Biostatistics, School of Public Health, Robert C. Byrd Health Sciences Center, West Virginia University, Morgantown, WV, 26505

Abstract

Enhanced sensitivity in echocardiographic analyses may allow for early detection of changes in cardiac function beyond the detection limits of conventional echocardiographic analyses, particularly in a small animal model. The goal of this study was to compare conventional echocardiographic measurements and speckle-tracking based strain imaging analyses in a small animal model of type 1 diabetes mellitus. Conventional analyses revealed differences in ejection fraction, fractional shortening, cardiac output, and stroke volume in diabetic animals relative to controls at 6-weeks post-diabetic onset. In contrast, when assessing short- and long-axis speckle-tracking based strain analyses, diabetic mice showed changes in average systolic radial strain, radial strain rate, radial displacement, and radial velocity, as well as decreased circumferential and longitudinal strain rate, as early as 1-week post-diabetic onset and persisting throughout the diabetic study. Further, we performed regional analyses for the LV and found that the free wall region was affected in both the short- and long-axis when assessing radial dimension parameters. These changes began 1-week post-diabetic onset and remained throughout the progression of the

Corresponding Author: John M. Hollander, Department of Exercise Physiology, West Virginia University School of Medicine, PO Box 9227, 1 Medical Center Drive, Morgantown, WV 26506, Tel: 1-(304) 293-3683, Fax: 1-(304) 293-7105, jhollander@hsc.wvu.edu.

Author Contributions

D.L.S., T.L.C., C.E.N., S.E.L., S.L.M. researched data. D.L.S., T.L.C., A.B.P., G.M.D., J.M.H. performed statistical analyses. D.L.S. wrote the manuscript. D.L.S., C.E.N., D.T., G.M.D., T.L.C., S.L.M., A.B.P., S.E.L., J.M.H. reviewed/edited manuscript. D.L.S., C.E.N., D.T., J.M.H. contributed to discussion.

Disclosures

None

disease. These findings demonstrate the use of speckle-tracking based strain as an approach to elucidate cardiac dysfunction from a global perspective, identifying left ventricular cardiac regions affected during the progression of type 1 diabetes mellitus earlier than contractile changes detected by conventional echocardiographic measurements.

Keywords

Echocardiography; Cardiac Function; Diabetic Cardiomyopathy; Strain Analysis; Speckle-tracking Imaging; Diabetes Mellitus

1.1 Introduction

Cardiac complications, such as diabetic cardiomyopathy, are the leading cause of mortality among diabetic patients [1, 2]. Diabetic cardiomyopathy is characterized by contractile abnormalities in the absence of coronary disease [1, 2]. The ability to assess cardiac performance within a clinical setting has been established in patients with coronary artery disease, myocardial infarction, and ischemic cardiomyopathy by numerous studies providing strain analyses [3–5]. Importantly, however, while this type of imaging and analysis has been utilized in the clinical setting, it is somewhat limited when considering small animal models of cardiovascular diseases [6–9]. Multiple methods for imaging cardiac performance noninvasively are available, but highly sensitive *in vivo* imaging is imperative for the assessment of cardiovascular dysfunction within small animal models. Evaluation of potential therapeutic treatments for diseases in small animal models is difficult without a way to critically assess cardiac function. Some treatments may elicit subtle beneficial or detrimental changes in cardiac function, undetectable with conventional echocardiographic assessment such as ejection fraction, emphasizing the importance of methods capable of detecting minute changes. Sensitive imaging analyses would afford the ability to detect cardiotoxic side effects of potential therapeutic treatments given for systemic pathological diseases. It would also allow investigators to assess the ability of pharmacological treatments for cardiovascular pathological disease states to subtly enhance contractile function. Until recently, the speckle-tracking based strain approach has been unavailable in small animal models because of the lack of highly sensitive imaging probes and software limitations preventing rapid assessment of cardiac performance. Bauer et al. suggested echocardiographic speckle-tracking based strain analyses as a way to quickly and accurately cardiac phenotype using an experimentally-induced myocardial infarction model [6]. Compared with conventional echocardiography, these authors found that speckle-tracking based strain analyses were capable of detecting subtle changes in myocardial deformation of the left ventricle (LV) [6]. Our current manuscript focuses on a type 1 diabetic mouse model, previously established to exhibit global cardiac dysfunction, which we hypothesize will be detected earlier using speckle-tracking based strain analyses compared to conventional analyses [10, 11]. Moreover, we aim to elucidate whether distinct regions of the LV develop dysfunction throughout the progression of type 1 diabetes mellitus, as well as decrements in global LV cardiac strain measurements, prior to the overt LV changes detected by conventional measurements. We describe the utility of using speckle-tracking based strain analyses to evaluate the progression of cardiac dysfunction in the type 1

diabetic heart. Comparing speckle-tracking based strain to conventional echocardiographic analyses, we found that analysis of strain allowed us to detect subtle changes much earlier during the progression of type 1 diabetes mellitus.

1.2 Research Design and Methods

1.2.1 Experimental Animals and Diabetes Induction

Animal experiments performed in this study conformed to the National Institutes of Health [12] Eighth Edition *Guidelines for the Care and Use of Laboratory Animals* and were approved by the West Virginia University Care and Use Committee. Male FVB mice were obtained from The Jackson Laboratory (Bar Harbor, Maine) at 4 weeks of age, placed on a standard diet, and received free access to water. Animals were housed in the West Virginia University Health Sciences Center animal facility on a 12-hour light/dark cycle in a temperature-controlled room. Type 1 diabetes mellitus was induced in 6-week-old mice using multiple low-dose streptozotocin (STZ) (Sigma, St. Louis, MO) injections. Briefly, mice were injected intraperitoneally after a 6-hour fasting period for 5 consecutive days with STZ at a dose of 50 mg/kg body weight dissolved in sodium citrate buffer (pH 4.5) [13, 14]. Hyperglycemia was confirmed one week post-injection by measuring blood glucose (Contour Blood Glucose test strips; Bayer, Mishawaka, IN), where >250 mg/dL was considered diabetic. One STZ injected animal was removed from the study. Animals were imaged at baseline prior to STZ injection, as well as at weeks 1, 3, and 6 after confirmation of type 1 diabetes mellitus.

1.2.2 Echocardiography

For echocardiographic assessment, each mouse was anesthetized in an induction chamber with inhalant isofluorane at 2.5% in 100% oxygen. When fully anesthetized, the mouse was transferred to dorsal recumbency, placed on a heated imaging platform, and maintained at 1% isofluorane for the duration of the experiment [15]. Electrode gel was applied to the limb leads allowing for an electrocardiogram and the respiration rate to be recorded during ultrasound imaging. A rectal probe was used to monitor the temperature of the mouse. Ultrasound images were acquired using a 32–55 MHz linear array transducer on the Vevo2100 Imaging System (Visual Sonics, Toronto, Canada). Placing the transducer to the left of the sternum allowed us to obtain images of the aortic outflow tract, the apex of the heart, and LV along its longest axis (i.e., long-axis B-mode images). Once all long-axis B-mode images were attained, the transducer was rotated 90 degrees to acquire short-axis B-mode images at the mid-papillary muscle level. Additionally, M-mode images were taken by placing a gate through the center of the short-axis B-mode images to obtain M-mode recordings of internal parameters of the myocardium. All images were acquired using the highest possible frame rate (233–401 frames/second) depending on the imaging axis to get the best possible image resolution for speckle-tracking based strain analyses. One trained individual in the West Virginia University Animal Models and Imaging Facility acquired all images.

1.2.3 Conventional Echocardiographic M-mode and Doppler Imaging

Conventional echocardiographic assessment was completed on grayscale M-mode parasternal short-axis images at the mid-papillary level of the LV (Figure 1A). Measurements obtained from LV M-mode images included end-diastolic and end-systolic diameters and volumes, anterior and posterior wall thickness at both systole and diastole, fractional shortening, ejection fraction, stroke volume, and cardiac output. LV volumes were automatically calculated by the Vevo2100 system when using M-mode imaging (Visual Sonics, Toronto, Canada). LV volume in systole (Volume;systole) was calculated by the program using the equation $(7.0 / (2.4 + \text{LVID;s})) \times \text{LVID;s}^3$), while LV volume in diastole (Volume;diastole) was calculated using the equation $(7.0 / (2.4 + \text{LVID;d})) \times \text{LVID;d}^3$) (Visual Sonics, Toronto, Canada). To calculate stroke volume for M-mode images, systolic volume was subtracted from diastolic volume (Visual Sonics, Toronto, Canada). All M-mode image measurements were calculated over three consecutive cardiac cycles and then averaged. As a measure of diastolic function, LV filling was assessed using Doppler echocardiography and measuring the E/A ratio, deceleration time, and Isovolumetric Relaxation Time (IVRT) over three cardiac cycles. The E/A ratio is a ratio of ventricular filling velocities of the early (E) peak to the late (A) peak of transmitral blood flow. Deceleration time of the E peak refers to the deceleration of blood flow through the mitral valve, while IVRT is the time from the closure of the aortic valve to the onset of mitral flow.

To assess reliability of the conventional measurements, each observer scored the parameter three times, and the average of the three observations was used for analysis on a subset of our study population (n=4). To determine intraobserver variability, the average coefficient of variance ((standard deviation/mean) × 100) was calculated for the observer for each measurement. The average coefficient of variance values for ejection fraction and E/A ratio were 3.4% and 1.3%, respectively. To determine both interobserver and test-retest intraobserver reliability, intra-class correlation (ICC) coefficients were calculated using a two-way mixed model with absolute agreement and reported in Table S1. Intraobserver test-retest reliability was calculated using values obtained at two separate time-points by a single rater. All ICC values for conventional measurements were greater than 0.8, indicating a high degree of both interobserver and intraobserver test-retest reliability [16]. When performing interobserver reproducibility measurements, the second observer selected and used the most appropriate image and frames to complete the strain measurements. All reported analyses in the manuscript used the Vevo2100 Imaging analysis software and included measurements from all animals for M-mode analyses (Visual Sonics, Toronto, Canada).

1.2.4 Speckle-tracking-based Strain Imaging Analyses

Based on concepts previously described, strain is defined as the change in the length of a segment divided by the original length of the segment and the strain rate as the rate at which this deformation occurs during a cardiac cycle [12, 17, 18]. Using the B-mode videos acquired from the parasternal short- and long-axes (Figure 1A), strain and strain rate were calculated for the radial, longitudinal, and circumferential dimensions with the Visual Sonics VevoStrain software (Toronto, Canada) using a speckle-tracking algorithm. Velocity and displacement were also calculated in both the long- and short-axes. Values generated by strain analyses were positive or negative depending on the assessed measurement. A positive

value for strain indicates fiber lengthening or thickening, such as in the radial dimension, while a negative value illustrates fiber shortening, in the circumferential or longitudinal dimensions [17, 19]. Briefly, B-mode video loops were chosen based upon image quality and the ability to visualize both the endocardial and epicardial wall borders, with limited interference by artifacts such as the sternum or lungs. Borders of the endocardium and epicardium were traced and checked throughout three cardiac cycles to ensure tracking was sufficient. Both the endocardial and epicardial borders were tracked through the image in a frame-by-frame manner by the software for measurements of strain, strain rate, velocity, and displacement. Strain analyses were performed, giving curvilinear data as output for both global and segmental values. Average peak global strain values were obtained from six independent anatomical segments of the LV. Global dyssynchrony for radial velocity, strain and strain rate were measured by using the standard deviation of time to peak strain, corrected for the RR interval [20, 21]. Further, segmental analyses were performed on short-axis images with the LV being split into the following regions: anterior free (AF), lateral (L), posterior (P), inferior free (IF), posterior septum (PS), and anterior septum (AS) (Figure 1B). Regional analyses were also performed on long-axis images with the LV divided into the following segments: anterior base (AB), anterior mid (AM), anterior apex (AA), posterior apex (PA), posterior mid (PM), and posterior base (PB) (Figure 1C). Because type 1 diabetes mellitus presents as a global dysfunction of LV parameters, segments were grouped into septal (AS and PS for short-axis; AA, AM, and AB for long-axis) and free wall (AF, L, P, and IF for short-axis; PA, PM, and PB for long-axis) regions for short- and long-axis in order to assess whether a particular section of the LV is affected during the progression of the disease. All individual regions were utilized during analyses and grouped as previously stated.

High intraobserver reproducibility was demonstrated on a subset of animals (n = 4) using speckle-tracking based strain measurements with a coefficient of variance equal to 6.1%, respectively. To determine both interobserver and test-retest intraobserver reliability, ICC coefficients were calculated using a two-way mixed model with absolute agreement and reported in Table S1. Interobserver and test-retest ICC values for strain were greater than 0.8, indicating a high degree of both interobserver and test-retest intraobserver reliability [16]. When performing interobserver reproducibility measurements, the second observer selected and used the most appropriate image and frames to complete the strain measurements. All reported analyses in the manuscript used the Vevo2100 Imaging analysis software (Visual Sonics, Toronto, Canada). One control and diabetic short-axis, along with one control long-axis image were excluded from strain measurements. In the short-axis, only still image pictures were collected and no movie loops; therefore, strain analyses could not be performed. For the excluded long-axis image, landmarks, such as the left atria and outflow track were not present; therefore, the movie loop was not used for strain analysis.

1.2.5 Statistical Analysis

All data are presented as mean ± standard error of the mean (SEM). Comparisons between control and diabetic animals were made within each given week to see whether changes were noted between the two groups using different types of echocardiographic analyses. Data were analyzed using a two-tailed Student’s t test to directly compare the type 1 diabetic

animals to the controls at a given time. $P < 0.05$ was considered statistically significant. Statistical analyses were performed using GraphPad Prism version 5.00 (GraphPad Software, San Diego, California).

1.3 Results

1.3.1 Conventional Echocardiographic Imaging and Analysis

To assess LV functional changes over time during type 1 diabetes, mice were imaged prior to diabetes induction (baseline) and at weeks 1, 3 and 6 after onset. Table 1 represents data collected from M-mode images at baseline and weeks 1, 3, and 6. M-mode images showed decreases in anterior and posterior wall thickness at diastole in diabetic animals as compared to controls 1-week post-diabetic onset (Table 1). At 3-weeks post-diabetic onset, decreased anterior and posterior wall thickness at diastole, as well as a decreased heart rate were noted in type 1 diabetic animals (Table 1). Six weeks after diabetes induction, overt LV dysfunction was present in the type 1 diabetic animals. Global function, assessed by conventional measures of echocardiography using M-mode images, showed decreased LV function in the type 1 diabetic animals at 6-weeks as compared to controls. Type 1 diabetes induced decreases in stroke volume, cardiac output, ejection fraction, and fractional shortening (Table 1). Further, type 1 diabetes caused decreases in diastolic diameter and volume, along with decreases in anterior and posterior wall thickness, indicative of myocardial remodeling (Table 1).

Representative Doppler images from control and type 1 diabetic animals illustrate a decreased E/A ratio in type 1 diabetic animals as compared to their controls at 6-weeks post-diabetic onset, with no changes occurring before this time point (Figure 2A–B). The decreased E/A ratio is due to the significantly decreased E wave at 6-weeks post-diabetic onset in the type 1 diabetic animals (Figure 2C). A decrease in the E wave, or early diastolic filling, could be a reflection of hemodynamic load, heart rate and/or cardiac output given the known dependence of the E/A ratio on these factors [22, 23]. The decreased E wave during type 1 diabetes is potentially due to a decreased ability for LV relaxation, while no changes were seen in the A wave (Figure 2D). E wave deceleration, a measure of how blood flow velocity declines during early diastole, was unchanged between control and type 1 diabetic animals throughout the course of our study (Figure 2E). IVRT, a measure of the time from the closure of the aortic valve to the onset of mitral flow, is increased in the type 1 diabetic animals 6-weeks post-diabetic onset (Figure 2F). Together, the echocardiography data indicate deficient systolic and diastolic LV function during type 1 diabetes mellitus predominantly being observed through conventional measures at 6-weeks post-diabetic onset.

1.3.2 Measures of Global Myocardial Performance During a Type I Diabetic Insult

Using the VevoStrain software to complete functional analyses for the LV, the complex pattern of deformation can be examined in the longitudinal, radial, and circumferential dimensions in both systole and diastole. Speckle-tracking based strain analyses trace the endocardium and epicardium frame-to-frame during the cine loop, providing assessment of the deformation of the tissue by using measurements of strain and strain rate in each of these

dimensions. Strain refers to the assessment of myocardial deformation, while strain rate measures the tissue velocity of deformation [17]. Global LV functional analyses, as well as the evaluation of six anatomic segments of the LV providing information on regional function, produce curvilinear data for strain analysis (Figure S1). Interestingly, speckle-tracking based strain analyses revealed differences as early as 1-week post-diabetic onset and persisting throughout the remainder of the study. Decreases in short-axis average systolic radial strain, strain rate, velocity, and displacement were noted in the type 1 diabetic animals at week 1 when compared to control animals, along with significantly decreased circumferential strain (Table 2). Three weeks post-diabetic onset, average systolic circumferential strain rate, radial strain, strain rate, velocity, and displacement were all significantly decreased in the diabetic animals as compared to controls (Table 2). Finally, at 6-weeks post-diabetic onset, decrements in average systolic circumferential strain rate, radial strain, strain rate, and velocity were noted in the type 1 diabetic animals when compared to controls (Table 2). No changes were noted in circumferential rate or displacement (Table 2). When assessing global diastolic strain measurements in the short-axis, radial strain was significantly decreased in diabetic animals when compared to controls starting at week 1 and persisting throughout the study (Table 2). Further, radial strain rate was decreased at weeks 3 and 6 post-diabetic onset (Table 2).

In the long-axis images, diabetic animals had decreased average systolic radial strain, strain rate, and velocity at weeks 1, 3 and 6 as compared to control within a given week (Table 3). Radial displacement was decreased at 1-week post-diabetic onset; however, this change was not observed throughout the rest of the study (Table 3). Further, longitudinal strain rate was decreased at weeks 3 and 6 post-diabetic onset; however, other longitudinal parameters such as strain, velocity, and displacement were unaltered during the progression of type 1 diabetes (Table 3). Average diastolic strain parameters were unchanged between control and diabetic animals in the long-axis (Table 3).

Systolic radial velocity, strain, and strain rate parameters, which were globally changing due to type 1 diabetes mellitus, were also analyzed for dyssynchrony in both the short- and long-axes. Type 1 diabetes mellitus was not associated with significant increases in global dyssynchrony for radial velocity, strain, and strain rate at any time point throughout the course of the study (Table S2).

Notably, it was discerned that changes in the short-axis, as seen by average myocardial systolic radial strain, strain rate, velocity, and displacement, as well as changes in circumferential strain rate occurred earlier than changes in LV function for conventional echocardiographic measurements. Further, radial strain and strain rate were also significantly decreased during diastole as early as 1-week post-diabetic onset. Similarly, decrements in average myocardial systolic radial measurements in the long-axis, along with longitudinal strain rate, were noted earlier during the progression of type 1 diabetes mellitus than measurements obtained by conventional echocardiography. This data provides evidence that global speckle-tracking-based strain analyses are capable of detecting early, subtle changes in LV function in the type 1 diabetic STZ mouse model in both systole and diastole.

1.3.3 Measures of Segmental Myocardial Performance During Type I Diabetes

Speckle-tracking based strain allows for the assessment of regional cardiac function by separating the LV into six distinct segments in both the short- and long-axes (Figure S1). Regional analyses were performed on short-axis images with the LV divided into the free wall (anterior free, lateral, posterior, and inferior free) and septal wall (posterior septum and anterior septum) regions (Figure 1B). Global strain analyses showed decreases in both short- and long-axis radial dimensions by deficient radial velocity, radial strain, and radial strain rate in the type 1 diabetic animals (Tables 2 and 3). When assessing these parameters using a regional approach in the short-axis, we found that radial velocity in the free wall and septal wall regions was decreased in the type 1 diabetic animals at weeks 1 and 3 (Figure 3A–B). Interestingly, only the free wall region of the LV was affected in the type 1 diabetic animals when looking at radial strain beginning at week 1 and remaining throughout the progression of type 1 diabetes, with no changes in the septal wall (Figure 3C–D). Finally, radial strain rate was also affected in both the free wall and septal wall regions of the LV (Figure 3E–F). Decreases in radial strain rate in the free wall occurred at week 1 and persisted throughout the study, while the septal wall was affected at weeks 3 and 6 post-diabetic onset (Figure 3E–F).

We also performed regional assessment on radial velocity, radial strain, and radial strain rate in the long-axis by separating the LV into free wall (posterior apex, posterior mid, and posterior base) and septal wall (anterior apex, anterior mid, and anterior base) regions (Figure 1C). Type 1 diabetic animals showed a decreased radial velocity in the free wall region of LV beginning at week 1 and persisting throughout the study, with only week 3 being affected in the septal wall region (Figure 4A–B). Radial strain was decreased in the free wall region of the type 1 diabetic animals at weeks 1, 3, and 6 post-diabetic onset, with no decrements in the septal wall region (Figure 4C–D). Finally, radial strain rate was decreased in the type 1 diabetic animals in the free wall region of the LV beginning 1-week post-diabetic onset and continuing throughout the progression of diabetes, while the septal wall region was only affected at week 3 (Figure 4E–F). Overall, regional assessment of the LV in the radial dimension showed that the free wall region in the short- and long-axis was predominantly affected during the progression of type 1 diabetes mellitus.

1.4 Discussion

This is the first application of echocardiographic speckle-tracking based strain analyses for cardiac phenotyping during the progression of type 1 diabetes in a mouse model. Here we describe the utility of using noninvasive echocardiographic analyses, such as speckle-tracking based strain, for early detection of LV dysfunction during the progression of type 1 diabetes mellitus.

The goal of this study was to provide a comparison between conventional echocardiographic measurements and speckle-tracking based strain analyses to see if changes in cardiac function would be detected earlier by means of more advanced methods. Further, we aimed to see if a particular region of the LV was predominantly affected during the progression of type 1 diabetes mellitus. The principal finding of this study was that speckle-tracking based strain analyses provided a sensitive approach to detect early global changes in LV function,

as compared to changes identified using conventional echocardiography during the development of diabetes mellitus in a type 1 diabetic mouse model. As early as 1-week post-diabetic onset, decreases in average systolic radial strain, radial strain rate, radial velocity, and radial displacement, along with circumferential and longitudinal strain rate at week 3 post-diabetic onset, were observed in short- and long-axis speckle-tracking based strain analyses and persisted throughout the study. Strain and strain rate were both found to be decreased in the radial axis at 1-week post-diabetic onset, indicating that myocardial deformation and the velocity at which that tissue deforms is impaired in this axis during the early stages of type 1 diabetes mellitus. Decreases in these systolic radial measurements are indicative of LV dysfunction allowing for subtle detection of early dysfunction occurring during type 1 diabetes mellitus [24]. Further, we found that the free wall region was predominantly affected in the radial dimension in both the short- and long-axis during type 1 diabetes mellitus. These findings highlight that the LV free wall could potentially be more affected than the septal wall during the progression of type 1 diabetes mellitus. These outcomes confirm other findings indicating that early changes are detected by speckle-tracking-based strain analysis prior to changes in conventional measurements giving investigators an approach to evaluate cardiac function in a small animal model with a cardiac pathology [6–9]. Additionally, speckle-tracking based strain analyses allow the ability to detect particular regions of the LV that may not be functioning properly. Finally, it provides investigators with the opportunity to assess the therapeutic benefit or detriment of treatment strategies on cardiac contractile function.

It is imperative in a clinical setting to be able to detect subtle changes in LV function and global heart function in order to intervene before the onset of a cardiac insult. Currently, clinical studies have shown that early detection of subtle changes in strain measurements were associated with the future development of cardiovascular disease, while conventional measures of cardiac structure and function were unaltered [25–32]. Though ejection fraction is typically the most prominent clinical measure for systolic dysfunction in the diabetic patient, strain and strain rate imaging have been shown to increase subclinical diabetic cardiomyopathy detection in patients [31, 33, 34]. Consequently, it is imperative that researchers using small animal models are able to detect these subtle and early changes in cardiac function in order to assess different cardiac therapies used to prevent cardiac dysfunction in the disease state. While strain measures have been utilized in clinical studies, experimental studies on small animal models were more complicated to perform due to fast heart rates, imaging equipment, and analysis software. However, advances such as high frame rates allowing for angle-independent measurements have permitted the adoption of strain analyses into an experimental setting, advancing the assessment of cardiac abnormalities and therapeutic approaches in small animal models of cardiovascular disease [27, 35, 36].

Because previous studies indicate that myocardial ischemia is associated with a dyssynchronous profile that undermines appropriate contractile function [9, 20, 21, 37], we assessed global dyssynchrony in a temporal fashion following type 1 diabetes mellitus induction. Our data indicated that the progression of the type 1 diabetic pathology through the initial six weeks was not associated with an increase in dyssynchrony. Our data are in contrast to others who have shown in models of myocardial infarction, impairments in

longitudinal and radial strain and strain rate parameters along with a concomitant increase in dyssynchrony [9, 20, 21, 37]. It is not entirely clear why the differences in findings occurred, though it may be a function of the different pathological models being studied. Specifically, these previous studies examined a focal cardiac region of tissue damage resulting from infarct, whereas our study in the diabetic heart reflect global dysfunction at an earlier pathological time point which may not be sufficient to induce an increase in dyssynchrony. Regardless, our current data suggests that dyssynchrony does not play a prominent role in cardiac pump function deficits during the initial progression of type 1 diabetes mellitus.

Speckle-tracking based strain allows for the separation of the LV into six distinct segments, permitting us to investigate regional cardiac dysfunction during the progression of type 1 diabetes mellitus. In this study, we found that the region predominantly affected in the radial dimension was the free wall in the short- and long-axis during the progression of type 1 diabetes mellitus. These findings highlight that the free wall of the LV could potentially be more affected than the septal wall during type 1 diabetes mellitus. This finding corroborates the potential use for regional assessment of the LV in myocardial function during type 1 diabetes, particularly via changes in the average systolic and diastolic radial measurements.

Our findings support the current literature stating that speckle-tracking based strain analysis possesses the potential for the sensitive evaluation of global and regional cardiac function [6, 17, 38, 39]. Studies of patients with acute heart failure and LV dysfunction concluded that strain powerfully predicted adverse cardiac events better than other conventional parameters, such as ejection fraction [40, 41]. In a swine model of heart failure with preserved ejection fraction, Hiemstra et al. showed decreases in systolic apical rotation rate, changes in strain measurements from longitudinal, radial, and circumferential axes, as well as strain rate changes all prior to the onset of increases in LV end diastolic pressure [39]. These results are in agreement with our findings, as this group found that speckle-tracking was capable of detecting early changes prior to the onset of overt LV impairment [39]. Bauer et al. found similar results in their assessment of a small animal model of myocardial infarction with the addition of ACE inhibitors [6]. Their principal findings concluded that speckle-tracking based strain was more sensitive than conventional echocardiographic measurements when assessing both the infarct region and the remote region, while subtle improvements were found in LV function in response to treatment with ACE inhibitors [6]. Additionally, in a recent study by the same group, they determined whether speckle-tracking based strain would provide insight regarding early changes in cardiac performance, prior to LV dysfunction seen by conventional echocardiography, during early stages of compensatory hypertrophic cardiac remodeling due to pressure overload [7]. These authors found regional myocardial dysfunction in a mouse model of pressure overload further illustrating the utility of using speckle-tracking based strain analyses, as well as regional assessment, in the characterization of early cardiac dysfunction that is not detectable by conventional echocardiographic measurements [7].

While standard echocardiographic techniques are useful in the evaluation of cardiac structure and function, they are often insensitive to subtle changes that occur early during the progression of cardiovascular disease preceding overt dysfunction. Previously, our

laboratory has reported changes in stroke volume, ejection fraction, fractional shortening and cardiac output due to type 1 diabetes mellitus; however, this current study offers a unique approach into pointing out a particular locale of dysfunction within the LV of the type 1 diabetic heart by implementing speckle-tracking based strain analysis [10, 11]. This study expounds upon current echocardiographic research providing evidence for using speckle-tracking based strain as an echocardiographic analysis software in small animal models of cardiovascular diseases [6, 7, 42–44]. It has been shown that speckle-tracking based strain analyses are highly sensitive compared to conventional measurements in small animal models, suggesting that these analyses could be used for the assessment of different therapeutic treatments for cardiovascular diseases or predisposing risk factors, including diabetes mellitus.

It is widely accepted that conventional measures of echocardiography are used to assess both cardiac structure, as well as function. However, the limitation for these types of measurements lies in the lack of sensitivity, which is overcome by the use of speckle-tracking based strain analyses. Although, limitations to this study exist even when using speckle-tracking based strain analyses and should be taken into consideration. The use of isofluorane, or any other anesthetic, is common in performing echocardiography on animals; however, it should be noted that anesthetics have the potential to alter the measurements recorded, though multiple studies have shown that even under anesthesia, echocardiographic measurements are reliable, particularly using speckle-tracking based strain analyses [45–47]. Although this is a concern because of the risk of causing a decrease in heart rate during image acquisition, heart rates recorded for the duration of this study remained near a physiological level. Literature notes that speckle tracking is heavily dependent upon 2D image quality, high frame rates, and angle dependency [18, 48]. To prevent variation, a single trained imaging technician acquired all images at the highest possible frame rate and avoided artifacts including the lungs and sternum. Other limitations such as out of plane motion and unknown software algorithms, known as filtering algorithms which calculate strain and strain rate values, are also important to keep in mind [17]. During a cardiac cycle the heart will move, sometimes causing speckles to move out of frame, making it difficult to surmise how the accuracy of speckle-tracking based strain analyses are affected [17]. Further, it is difficult to compare filtering algorithms between different software vendors and between the analyses, inherently posing another limitation [17]. Variability in the assessment of strain has also been addressed within the literature [49, 50]. As in the study performed by Hiemstra et al., we observed variation between our time points, which could potentially be due to the methodology used, but also because of animal maturation and normal physiological growth over the duration of the study [39]. Indeed, we previously reported differences in heart weights, 6 weeks following STZ induction, which may be a function of animal growth and pathology development that may have occurred similarly in the current study [10, 51]. With that being said, it is important to note that the goal of the present study was to determine whether speckle-tracking based strain analyses could identify cardiac dysfunction at a given time point, earlier than conventional measures, as opposed to across time points, limiting concern for serial assessment. Further, it is crucial to do a longer period of study to see if parameters of stress/strain are transient and/or worsen during type 1 diabetes at a longer duration. As others have previously shown, strain is dependent on a

number of factors, such as complexity of myocardial fiber orientation, which could potentially include the evaluation of different fiber layers at a diverse number of levels leading to variation in results [6, 39, 52]. Because of this, we decided that the question of interest was to find out if certain echocardiographic parameters were capable of detecting changes in LV function earlier during the progression of type 1 diabetes mellitus. Therefore, we chose to not include the serial change, but instead evaluate different echocardiographic parameters at each time point individually.

One question raised by the current study regards what mechanisms contribute to the observed changes in cardiac strain parameters? Of note are our findings of decreased radial strain during diastole which in combination with reduced early diastolic filling (decreased E), decreased end diastolic volume, and increased IVRT, suggest that impaired filling may be involved in the decreased stroke volume observed and ultimately, reduced cardiac output following diabetic insult. Since reduced E and IVRT typically reflect early filling, impaired energetics leading to increased time to reuptake calcium or trouble breaking cross-bridges during early diastole may be mechanistic contributors to changes in strain parameters. Because these processes are ATP-dependent, any bioenergetic compromise in the mitochondrion's ability to provide an adequate supply of ATP could have an effect on strain dynamics. Indeed, we have previously reported compromised mitochondrial function and ATP-generating capacity during type 1 diabetes mellitus [10, 51, 53]. Taken together, mitochondrial dysfunction in the face of type 1 diabetes mellitus may provide a mechanistic link between altered bioenergetic function and changes cardiac strain dynamics.

During normal LV function the heart deforms to show myocardial thickening and thinning via the radial axis, as well as shortening and lengthening in the longitudinal and circumferential axes, depending on whether the heart is in systole or diastole [17]. Alterations in the deformation of the myocardium, revealed by strain measurements, are the earliest noninvasive indicators for the development of cardiac dysfunction [54, 55]. We demonstrate the advantage of using speckle-tracking based strain analyses to detect changes in LV function earlier than conventional echocardiographic measurements. While the correlation between contractile complications and diabetic cardiomyopathy have been well established, the results presented in this study reveal how early detection via strain measurements has the potential to play a critical role in evaluating therapeutic treatments for contractile dysfunction in the diabetic heart.

Supplementary Material

Refer to Web version on PubMed Central for supplementary material.

Acknowledgments

The authors would like to thank the WVU Animal Models and Imaging Facility for all of the echocardiographic images, which has been supported by the Mary Babb Randolph Cancer Center and NIH grants P20 RR016440, P30 GM103488 and S10 RR026378. This work was supported by NIH DP2DK083095 (J.M.H.), NIH R56 HL128485 (J.M.H.), NIH T32HL090610 (T.L.C., D.L.S.), AHA-14PRE19890020 (D.L.S.), AHA-13PRE16850066 (C.E.N.), DGE-1144676 (C.E.N.) and WVU CTSI (NIH U54GM104942).

References

1. Kannel WB, McGee DL. Diabetes and cardiovascular disease. The Framingham study. JAMA : the journal of the American Medical Association. 1979; 241:2035–8. [PubMed: 430798]
2. Zarich SW, Nesto RW. Diabetic cardiomyopathy. American heart journal. 1989; 118:1000–12. [PubMed: 2683698]
3. Blondheim DS, Kazatsker M, Friedman Z, Lysyansky P, Meisel SR, Asif A, et al. Effect of medical therapy for heart failure on segmental myocardial function in patients with ischemic cardiomyopathy. The American journal of cardiology. 2007; 99:1741–4. [PubMed: 17560886]
4. Chen J, Cao T, Duan Y, Yuan L, Yang Y. Velocity vector imaging in assessing the regional systolic function of patients with post myocardial infarction. Echocardiography. 2007; 24:940–5. [PubMed: 17894572]
5. Liang HY, Cauduro S, Pellikka P, Wang J, Urheim S, Yang EH, et al. Usefulness of two-dimensional speckle strain for evaluation of left ventricular diastolic deformation in patients with coronary artery disease. The American journal of cardiology. 2006; 98:1581–6. [PubMed: 17145214]
6. Bauer M, Cheng S, Jain M, Ngoy S, Theodoropoulos C, Trujillo A, et al. Echocardiographic speckle-tracking based strain imaging for rapid cardiovascular phenotyping in mice. Circ Res. 2011; 108:908–16. [PubMed: 21372284]
7. Bauer M, Cheng S, Unno K, Lin FC, Liao R. Regional cardiac dysfunction and dyssynchrony in a murine model of afterload stress. PloS one. 2013; 8:e59915. [PubMed: 23560059]
8. Kovacs A, Olah A, Lux A, Matyas C, Nemeth BT, Kellermayer D, et al. Strain and strain rate by speckle-tracking echocardiography correlate with pressure-volume loop-derived contractility indices in a rat model of athlete's heart. Am J Physiol Heart Circ Physiol. 2015; 308:H743–8. [PubMed: 25617359]
9. Yamada S, Arrell DK, Kane GC, Nelson TJ, Perez-Terzic CM, Behfar A, et al. Mechanical dyssynchrony precedes QRS widening in ATP-sensitive K(+) channel-deficient dilated cardiomyopathy. J Am Heart Assoc. 2013; 2:e000410. [PubMed: 24308936]
10. Baseler WA, Dabkowski ER, Jagannathan R, Thapa D, Nichols CE, Shepherd DL, et al. Reversal of mitochondrial proteomic loss in Type 1 diabetic heart with overexpression of phospholipid hydroperoxide glutathione peroxidase. Am J Physiol Regul Integr Comp Physiol. 2013; 304:R553–65. [PubMed: 23408027]
11. Thapa D, Nichols CE, Lewis SE, Shepherd DL, Jagannathan R, Croston TL, et al. Transgenic overexpression of mitofilin attenuates diabetes mellitus-associated cardiac and mitochondria dysfunction. J Mol Cell Cardiol. 2015; 79:212–23. [PubMed: 25463274]
12. Pavlopoulos H, Nihoyannopoulos P. Strain and strain rate deformation parameters: from tissue Doppler to 2D speckle tracking. The international journal of cardiovascular imaging. 2008; 24:479–91. [PubMed: 18074240]
13. Inada A, Kanamori H, Arai H, Akashi T, Araki M, Weir GC, et al. A model for diabetic nephropathy: advantages of the inducible cAMP early repressor transgenic mouse over the streptozotocin-induced diabetic mouse. Journal of cellular physiology. 2008; 215:383–91. [PubMed: 18270980]
14. Kim E, Sohn S, Lee M, Jung J, Kineman RD, Park S. Differential responses of the growth hormone axis in two rat models of streptozotocin-induced insulinopenic diabetes. The Journal of endocrinology. 2006; 188:263–70. [PubMed: 16461552]
15. James JF, Hewett TE, Robbins J. Cardiac physiology in transgenic mice. Circ Res. 1998; 82:407–15. [PubMed: 9506700]
16. Altman, DG. Practical Statistics for Medical Research. London: Chapman and Hall; 1991.
17. Blessberger H, Binder T. Two dimensional speckle tracking echocardiography: clinical applications. Heart. 2010; 96:2032–40. [PubMed: 21088126]
18. D'Hooge J, Heimdal A, Jamal F, Kukulski T, Bijnens B, Rademakers F, et al. Regional strain and strain rate measurements by cardiac ultrasound: principles, implementation and limitations. Eur J Echocardiogr. 2000; 1:154–70. [PubMed: 11916589]

19. Marwick TH. Measurement of strain and strain rate by echocardiography: ready for prime time? J Am Coll Cardiol. 2006; 47:1313–27. [PubMed: 16580516]
20. Bhan A, Sirker A, Zhang J, Protti A, Catibog N, Driver W, et al. High-frequency speckle tracking echocardiography in the assessment of left ventricular function and remodeling after murine myocardial infarction. Am J Physiol Heart Circ Physiol. 2014; 306:H1371–83. [PubMed: 24531814]
21. Yu CM, Gorcsan J 3rd, Bleeker GB, Zhang Q, Schalij MJ, Suffoletto MS, et al. Usefulness of tissue Doppler velocity and strain dyssynchrony for predicting left ventricular reverse remodeling response after cardiac resynchronization therapy. The American journal of cardiology. 2007; 100:1263–70. [PubMed: 17920368]
22. Hill JC, Palma RA. Doppler tissue imaging for the assessment of left ventricular diastolic function: a systematic approach for the sonographer. J Am Soc Echocardiogr. 2005; 18:80–8. quiz 9. [PubMed: 15637496]
23. Nagueh SF, Appleton CP, Gillebert TC, Marino PN, Oh JK, Smiseth OA, et al. Recommendations for the evaluation of left ventricular diastolic function by echocardiography. J Am Soc Echocardiogr. 2009; 22:107–33. [PubMed: 19187853]
24. Hashimoto I, Li X, Hejmadi Bhat A, Jones M, Zetts AD, Sahn DJ. Myocardial strain rate is a superior method for evaluation of left ventricular subendocardial function compared with tissue Doppler imaging. J Am Coll Cardiol. 2003; 42:1574–83. [PubMed: 14607441]
25. Cottrell C, Kirkpatrick JN. Echocardiographic strain imaging and its use in the clinical setting. Expert review of cardiovascular therapy. 2010; 8:93–102. [PubMed: 20030024]
26. Mondillo S, Galderisi M, Mele D, Cameli M, Lomoriello VS, Zaca V, et al. Speckle-tracking echocardiography: a new technique for assessing myocardial function. Journal of ultrasound in medicine : official journal of the American Institute of Ultrasound in Medicine. 2011; 30:71–83. [PubMed: 21193707]
27. Leung DY, Ng AC. Emerging clinical role of strain imaging in echocardiography. Heart, lung & circulation. 2010; 19:161–74.
28. Ernande L, Bergerot C, Girerd N, Thibault H, Davidsen ES, Gautier Pignon-Blanc P, et al. Longitudinal myocardial strain alteration is associated with left ventricular remodeling in asymptomatic patients with type 2 diabetes mellitus. J Am Soc Echocardiogr. 2014; 27:479–88. [PubMed: 24508363]
29. Ernande L, Rietzschel ER, Bergerot C, De Buyzere ML, Schnell F, Groisne L, et al. Impaired myocardial radial function in asymptomatic patients with type 2 diabetes mellitus: a speckle-tracking imaging study. J Am Soc Echocardiogr. 2010; 23:1266–72. [PubMed: 20932716]
30. Fang ZY, Leano R, Marwick TH. Relationship between longitudinal and radial contractility in subclinical diabetic heart disease. Clin Sci (Lond). 2004; 106:53–60. [PubMed: 12924982]
31. Fang ZY, Yuda S, Anderson V, Short L, Case C, Marwick TH. Echocardiographic detection of early diabetic myocardial disease. J Am Coll Cardiol. 2003; 41:611–7. [PubMed: 12598073]
32. Nakai H, Takeuchi M, Nishikage T, Lang RM, Otsuji Y. Subclinical left ventricular dysfunction in asymptomatic diabetic patients assessed by two-dimensional speckle tracking echocardiography: correlation with diabetic duration. Eur J Echocardiogr. 2009; 10:926–32. [PubMed: 19622532]
33. Boyer JK, Thanigaraj S, Schechtman KB, Perez JE. Prevalence of ventricular diastolic dysfunction in asymptomatic, normotensive patients with diabetes mellitus. The American journal of cardiology. 2004; 93:870–5. [PubMed: 15050491]
34. Muranaka A, Yuda S, Tsuchihashi K, Hashimoto A, Nakata T, Miura T, et al. Quantitative assessment of left ventricular and left atrial functions by strain rate imaging in diabetic patients with and without hypertension. Echocardiography. 2009; 26:262–71. [PubMed: 19017317]
35. Peng Y, Popovic ZB, Sopko N, Drinko J, Zhang Z, Thomas JD, et al. Speckle tracking echocardiography in the assessment of mouse models of cardiac dysfunction. Am J Physiol Heart Circ Physiol. 2009; 297:H811–20. [PubMed: 19561310]
36. Mor-Avi V, Lang RM, Badano LP, Belohlavek M, Cardim NM, Derumeaux G, et al. Current and evolving echocardiographic techniques for the quantitative evaluation of cardiac mechanics: ASE/EAE consensus statement on methodology and indications endorsed by the Japanese Society of Echocardiography. J Am Soc Echocardiogr. 2011; 24:277–313. [PubMed: 21338865]

37. Yamada S, Nelson TJ, Kane GC, Martinez-Fernandez A, Crespo-Diaz RJ, Ikeda Y, et al. Induced pluripotent stem cell intervention rescues ventricular wall motion disparity, achieving biological cardiac resynchronization post-infarction. J Physiol. 2013; 591:4335–49. [PubMed: 23568891]
38. Ram R, Mickelsen DM, Theodoropoulos C, Blaxall BC. New approaches in small animal echocardiography: imaging the sounds of silence. Am J Physiol Heart Circ Physiol. 2011; 301:H1765–80. [PubMed: 21873501]
39. Hiemstra JA, Liu S, Ahlman MA, Schuleri KH, Lardo AC, Baines CP, et al. A new twist on an old idea: a two-dimensional speckle tracking assessment of cyclosporine as a therapeutic alternative for heart failure with preserved ejection fraction. Physiological reports. 2013; 1:e00174. [PubMed: 24744855]
40. Cho GY, Marwick TH, Kim HS, Kim MK, Hong KS, Oh DJ. Global 2-dimensional strain as a new prognosticator in patients with heart failure. J Am Coll Cardiol. 2009; 54:618–24. [PubMed: 19660692]
41. Mignot A, Donal E, Zaroui A, Reant P, Salem A, Hamon C, et al. Global longitudinal strain as a major predictor of cardiac events in patients with depressed left ventricular function: a multicenter study. J Am Soc Echocardiogr. 2010; 23:1019–24. [PubMed: 20810243]
42. Popovic ZB, Benejam C, Bian J, Mal N, Drinko J, Lee K, et al. Speckle-tracking echocardiography correctly identifies segmental left ventricular dysfunction induced by scarring in a rat model of myocardial infarction. Am J Physiol Heart Circ Physiol. 2007; 292:H2809–16. [PubMed: 17277023]
43. Thibault H, Gomez L, Donal E, Augeul L, Scherrer-Crosbie M, Ovize M, et al. Regional myocardial function after myocardial infarction in mice: a follow-up study by strain rate imaging. J Am Soc Echocardiogr. 2009; 22:198–205. [PubMed: 19121566]
44. Thibault H, Gomez L, Donal E, Pontier G, Scherrer-Crosbie M, Ovize M, et al. Acute myocardial infarction in mice: assessment of transmurality by strain rate imaging. Am J Physiol Heart Circ Physiol. 2007; 293:H496–502. [PubMed: 17384134]
45. Rottman JN, Ni G, Brown M. Echocardiographic evaluation of ventricular function in mice. Echocardiography. 2007; 24:83–9. [PubMed: 17214630]
46. Roth DM, Swaney JS, Dalton ND, Gilpin EA, Ross J Jr. Impact of anesthesia on cardiac function during echocardiography in mice. Am J Physiol Heart Circ Physiol. 2002; 282:H2134–40. [PubMed: 12003821]
47. Wu J, Bu L, Gong H, Jiang G, Li L, Ma H, et al. Effects of heart rate and anesthetic timing on high-resolution echocardiographic assessment under isoflurane anesthesia in mice. Journal of ultrasound in medicine : official journal of the American Institute of Ultrasound in Medicine. 2010; 29:1771–8. [PubMed: 21098849]
48. Geyer H, Caracciolo G, Abe H, Wilansky S, Carerj S, Gentile F, et al. Assessment of myocardial mechanics using speckle tracking echocardiography: fundamentals and clinical applications. J Am Soc Echocardiogr. 2010; 23:351–69. quiz 453-5. [PubMed: 20362924]
49. Marwick TH. Will standardization make strain a standard measurement? J Am Soc Echocardiogr. 2012; 25:1204–6. [PubMed: 23089621]
50. Oxborough D, George K, Birch KM. Intraobserver reliability of two-dimensional ultrasound derived strain imaging in the assessment of the left ventricle, right ventricle, and left atrium of healthy human hearts. Echocardiography. 2012; 29:793–802. [PubMed: 22506912]
51. Dabkowski ER, Williamson CL, Bukowski VC, Chapman RS, Leonard SS, Peer CJ, et al. Diabetic cardiomyopathy-associated dysfunction in spatially distinct mitochondrial subpopulations. Am J Physiol Heart Circ Physiol. 2009; 296:H359–69. [PubMed: 19060128]
52. Risum N, Ali S, Olsen NT, Jons C, Khouri MG, Lauridsen TK, et al. Variability of global left ventricular deformation analysis using vendor dependent and independent two-dimensional speckle-tracking software in adults. J Am Soc Echocardiogr. 2012; 25:1195–203. [PubMed: 22981228]
53. Dabkowski ER, Williamson CL, Hollander JM. Mitochondria-specific transgenic overexpression of phospholipid hydroperoxide glutathione peroxidase (GPx4) attenuates ischemia/reperfusion-associated cardiac dysfunction. Free Radic Biol Med. 2008; 45:855–65. [PubMed: 18638546]

54. Mizuguchi Y, Oishi Y, Miyoshi H, Iuchi A, Nagase N, Oki T. The functional role of longitudinal, circumferential, and radial myocardial deformation for regulating the early impairment of left ventricular contraction and relaxation in patients with cardiovascular risk factors: a study with two-dimensional strain imaging. J Am Soc Echocardiogr. 2008; 21:1138–44. [PubMed: 18926389]

55. Wang J, Khoury DS, Yue Y, Torre-Amione G, Nagueh SF. Preserved left ventricular twist and circumferential deformation, but depressed longitudinal and radial deformation in patients with diastolic heart failure. Eur Heart J. 2008; 29:1283–9. [PubMed: 18385117]

Highlights

- Conventional measurements were decreased at 6-weeks post-diabetic onset.
- Diastolic dysfunction was seen at 6-weeks post-diabetic onset.
- Myocardial strain dysfunction was noted as early as 1-week post-diabetic onset.
- Posterior and free wall regions of LV show dysfunction throughout diabetes.
- Strain analyses allow for early detection of myocardial dysfunction during diabetes.

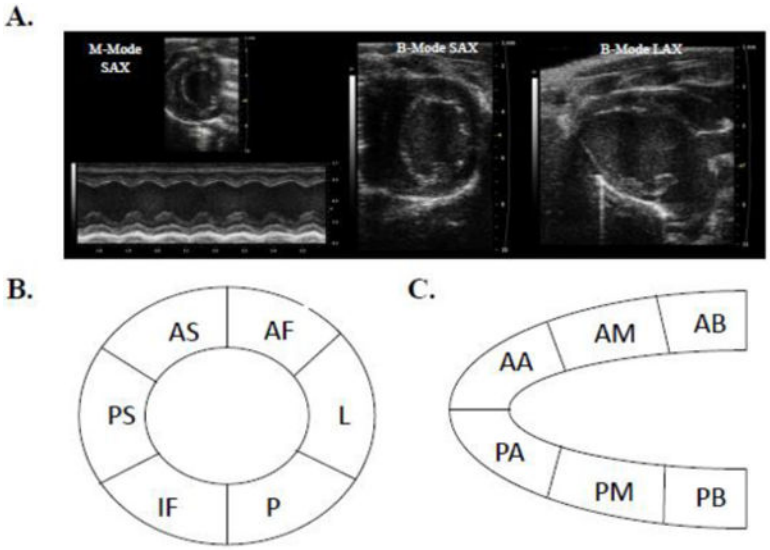

Figure 1. Echocardiography and speckle-tracking-based strain

Representative M-mode and B-mode control mouse echocardiographic images from which conventional analyses and speckle-tracking-based strain analyses were performed (**A**). A schematic of myocardial regions identified form the parasternal short-axis view (**B**) and long-axis view (**C**). SAX indicates short-axis; AF, anterior free; L, lateral; P, posterior; IF, inferior free (AF, L, P, and IF considered the free wall region); PS, posterior septum; AS, anterior septum (PS and AS considered the septal wall region). LAX indicates long-axis; AB, anterior base; AM, anterior mid; AA, anterior apex (AB, AM, and AA considered the septal wall region); PA, posterior apex; PM, posterior mid; PB, posterior base (PA, PM, and PB considered the free wall region).

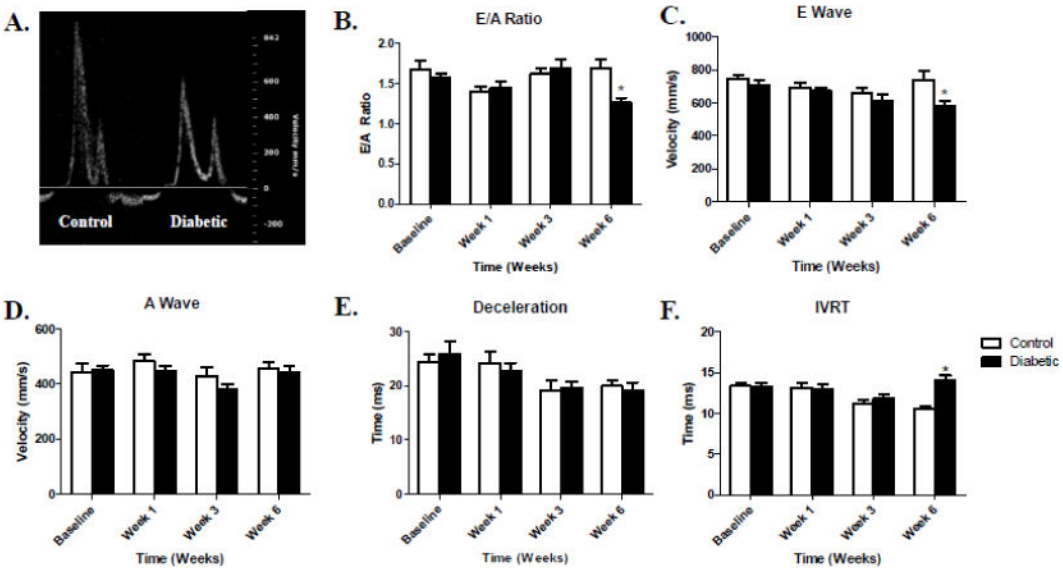

Figure 2. Color Doppler Imaging for Diastolic Function

Comparative color Doppler images between control (left) and diabetic (right) mice 6-weeks post-diabetic onset **(A)**. E/A ratio data during type 1 diabetes mellitus progression **(B)**. E wave velocity over time during type 1 diabetes mellitus (**C**). A wave velocity over time during type 1 diabetes mellitus (**D**). Deceleration time (**E**) and Isovolumetric Relaxation Time (IVRT) during the progression of type 1 diabetes mellitus (**F**). Values are means ± SEM. **P* < 0.05 as compared to control at a given time. Open bars = Control animals, *n* = 8; Closed bars = Diabetic animals, *n* = 8.

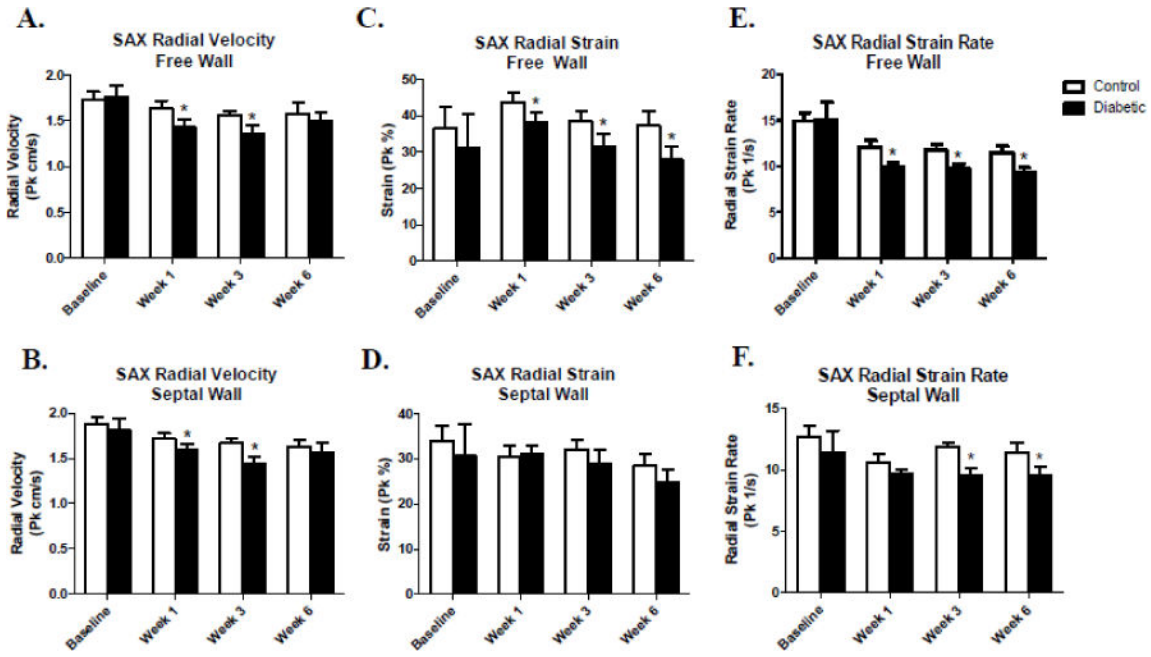

Figure 3. Regional assessment of systolic radial velocity, radial strain, and radial strain rate via speckle-tracking based strain analysis in the short-axis

Comparison of control and type 1 diabetic animals assessing systolic radial velocity, radial strain, and radial strain rate between free wall and septal wall segments of the LV within a given week **(A–F)**. Values are means ± SEM; **P* < 0.05 as compared to control within a given week. Open bars = Control animals, *n* = 8; Closed bars = Diabetic animals, *n* = 8. Free wall segments include the anterior free wall, lateral, posterior, and inferior free wall. Septal wall segments include the anterior septum and posterior septum.

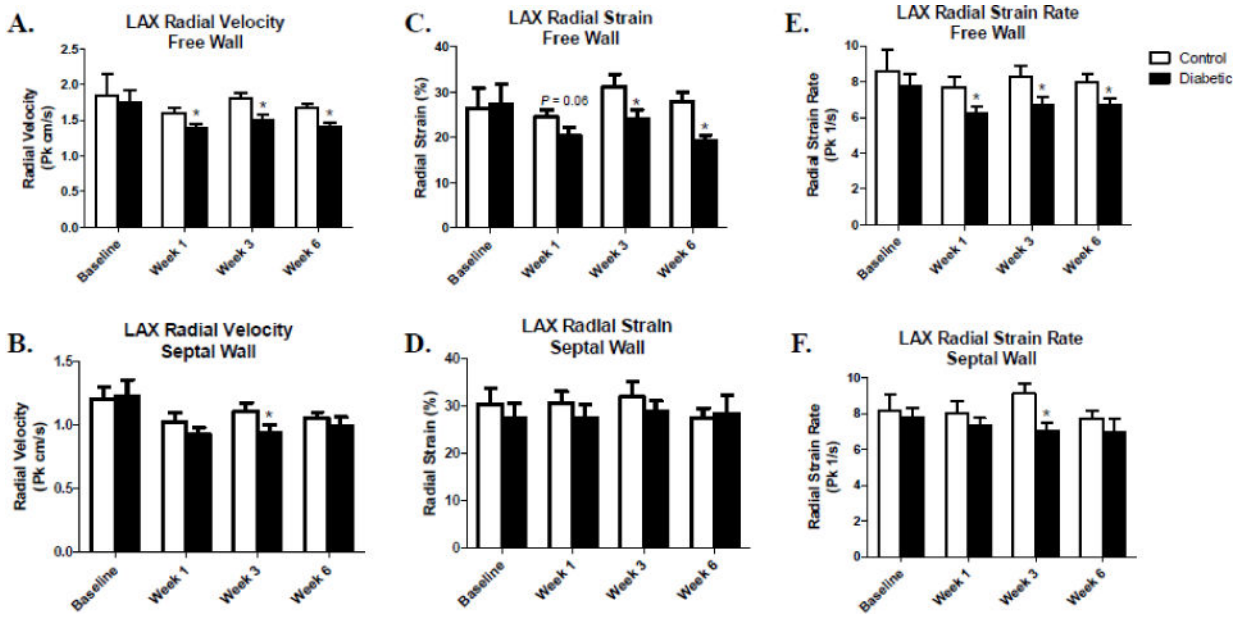

Figure 4. Regional assessment of systolic radial velocity, radial strain, and radial strain rate via speckle-tracking-based strain analysis in the long-axis

Comparison of control and type 1 diabetic animals assessing systolic radial velocity, radial strain, and radial strain rate between free wall and septal wall segments of the LV within a given week **(A–F)**. Values are means ± SEM; **P* < 0.05 as compared to control within a given week. Open bars = Control animals, *n* = 8; Closed bars = Diabetic animals, *n* = 8. Septal wall segments include the anterior base, anterior mid, and anterior apex. Free wall segments include the posterior base, posterior mid, and posterior apex.

Table 1

Conventional echocardiographic characteristics.

	Baseline		Week 1		Week 3		Week 6	
M-mode	**Control**	**Diabetic**	**Control**	**Diabetic**	**Control**	**Diabetic**	**Control**	**Diabetic**
Heart rate (bpm)	418.4 ± 20.9	431.3 ± 14.8	484.0 ± 21.0	457.2 ± 11.9	503.2 ± 11.5	448.4 ± 17.5*	498.5 ± 12.1	494.5 ± 12.1
Stroke volume (μL)	33.6 ± 2.5	33.0 ± 2.0	30.6 ± 2.4	29.6 ± 1.6	26.7 ± 1.2	25.8 ± 2.5	30.0 ± 1.9	21.0 ± 1.8*
Ejection fraction (%)	75.3 ± 0.9	74.4 ± 1.4	72.3 ± 1.5	68.6 ± 1.5	71.2 ± 1.3	68.2 ± 3.0	70.9 ± 1.8	65.0 ± 1.7*
Fractional shortening (%)	42.3 ± 1.0	42.3 ± 1.3	40.5 ± 1.3	37.5 ± 1.1	39.6 ± 1.2	37.4 ± 2.3	39.5 ± 1.7	34.4 ± 1.3*
Cardiac output (mL/min)	14.0 ± 1.0	13.7 ± 1.3	14.9 ± 1.5	13.4 ± 0.7	13.2 ± 0.6	11.4 ± 1.1	14.9 ± 0.7	10.3 ± 1.0*
Diameter; systole (mm)	1.8 ± 0.1	1.7 ± 0.1	1.9 ± 0.1	2.1 ± 0.1	1.8 ± 0.06	1.9 ± 0.2	2.0 ± 0.1	1.9 ± 0.1
Diameter; diastole (mm)	3.3 ± 0.1	3.2 ± 0.1	3.2 ± 0.1	3.3 ± 0.1	3.0 ± 0.05	3.1 ± 0.2	3.2 ± 0.1	2.9 ± 0.1*
Volume;systole (μL)	9.4 ± 0.1	10.6 ± 1.0	12.1 ± 1.2	15.3 ± 1.4	10.4 ± 0.8	13.7 ± 2.9	12.6 ± 1.5	11.5 ± 1.4
Volume;diastole (μL)	43.0 ± 3.4	40.4 ± 2.8	42.7 ± 3.3	44.9 ± 2.7	35.6 ± 1.4	39.5 ± 5.1	42.6 ± 3.2	32.5 ± 3.0*
Anterior wall thickness; systole (mm)	1.7 ± 0.07	1.5 ± 0.09	1.4 ± 0.07	1.4 ± 0.03	1.5 ± 0.05	1.4 ± 0.04	1.5 ± 0.04	1.5 ± 0.03
Anterior wall thickness; diastole (mm)	1.1 ± 0.05	1.1 ± 0.1	1.2 ± 0.04	1.0 ± 0.05*	1.2 ± 0.06	1.0 ± 0.06*	1.0 ± 0.03	0.9 ± 0.03*
Posterior wall thickness; systole (mm)	1.1 ± 0.05	1.1 ± 0.08	1.1 ± 0.04	1.2 ± 0.05	1.3 ± 0.06	1.2 ± 0.05	1.4 ± 0.1	1.3 ± 0.05
Posterior wall thickness; diastole (mm)	0.8 ± 0.03	0.9 ± .0.4	1.1 ± 0.06	0.8 ± 0.05*	1.0 ± 0.03	0.8 ± 0.05*	1.0 ± 0.04	0.8 ± 0.03*

Values are shown as means ± SEM.

*$P < 0.05$ Control versus Diabetic in a given week. 2-tailed Student's t test. Control $n = 8$, Diabetic $n = 8$.

Table 2

Average short-axis (SAX) systolic and diastolic strain echocardiographic characteristics.

	Baseline		Week 1		Week 3		Week 6	
	Control	**Diabetic**	**Control**	**Diabetic**	**Control**	**Diabetic**	**Control**	**Diabetic**
SAX strain measurements at systole								
Circumferential strain (%)	− 32.9 ± 1.4	− 33.6 ± 1.8	− 31.2 ± 1.1	− 28.5 ± 0.5*	− 29.0 ± 0.9	− 27.8 ± 1.4	− 29.4 ± 1.5	− 26.8 ± 1.8
Circumferential SR (1/s)	− 13.7 ± 1.0	− 13.8 ± 1.1	− 12.8 ± 0.6	− 11.6 ± 0.9	− 13.3 ± 0.5	− 10.9 ± 0.8*	− 12.1 ± 0.4	− 11.6 ± 1.5*
Circumferential rotation rate (deg/s)	340.3 ± 27.5	342.7 ± 34.6	280.4 ± 18.6	270.2 ± 15.7	320.2 ± 33.5	321.9 ± 24.2	318.9 ± 37.6	347.4 ± 31.0
Circumferential displacement (deg)	4.0 ± 0.5	3.6 ± 0.7	3.2 ± 0.4	3.3 ± 0.3	4.4 ± 0.8	4.7 ± 0.5	4.1 ± 0.6	4.5 ± 0.7
Radial strain (%)	35.8 ± 2.0	35.1 ± 2.9	37.4 ± 0.8	34.0 ± 1.3*	35.5 ± 0.9	30.5 ± 2.1*	33.7 ± 0.8	25.7 ± 1.8*
Radial SR (1/s)	12.8 ± 0.5	12.8 ± 1.0	11.8 ± 0.6	10.1 ± 0.4*	11.8 ± 0.3	10.0 ± 0.4*	11.3 ± 0.6	9.8 ± 0.4*
Radial velocity (cm/s)	1.7 ± 0.07	1.8 ± 0.1	1.6 ± 0.06	1.5 ± 0.05*	1.6 ± 0.04	1.4 ± 0.07*	1.6 ± 0.08	1.4 ± 0.09*
Radial displacement (mm)	0.57 ± 0.01	0.61 ± 0.05	0.55 ± 0.02	0.48 ± 0.02*	0.53 ± 0.01	0.44 ± 0.01*	0.52 ± 0.02	0.48 ± 0.04
SAX strain measurements at diastole								
Circumferential strain (%)	1.5 ± 0.8	2.0 ± 0.5	1.5 ± 0.2	1.4 ± 0.3	2.0 ± 0.4	2.1 ± 0.3	1.9 ± 0.4	2.2 ± 0.2
Circumferential SR (1/s)	24.3 ± 1.6	22.9 ± 2.3	16.4 ± 0.6	17.5 ± 0.8	15.4 ± 0.4	16.2 ± 1.1	17.4 ± 1.2	17.3 ± 1.2
Circumferential rotation rate (deg/s)	− 391.5 ± 32.0	− 408.3 ± 43.8	− 362.7 ± 20.0	− 382.4 ± 24.7	− 401.5 ± 26.3	− 421.5 ± 32.6	361.0 ± 33.5	− 395.5 ± 28.9
Circumferential displacement (deg)	− 3.8 ± 0.7	− 3.8 ± 0.5	− 3.8 ± 0.7	− 2.5 ± 0.3	− 2.1 ± 0.5	− 2.4 ± 0.4	− 2.8 ± 0.6	− 3.0 ± 0.4
Radial strain (%)	− 2.4 ± 0.4	− 3.9 ± 0.9	− 2.3 ± 0.2	− 1.6 ± 0.3*	− 3.7 ± 0.5	− 2.0 ± 0.4*	− 3.8 ± 0.7	− 2.0 ± 0.5*
Radial SR (1/s)	− 15.8 ± 0.9	− 16.6 ± 2.1	− 13.3 ± 0.9	− 12.5 ± 0.5	− 13.1 ± 0.3	− 11.2 ± 0.5*	− 13.7 ± 0.7	− 11.1 ± 0.9*
Radial velocity (cm/s)	− 2.7 ± 0.2	− 2.4 ± 0.3	− 1.9 ± 0.08	− 1.9 ± 0.1	− 1.8 ± 0.07	− 1.7 ± 0.1	− 2.0 ± 0.1	− 1.7 ± 0.2
Radial displacement (mm)	− 0.007 ± 0.002	− 0.008 ± 0.002	− 0.01 ± 0.003	− 0.02 ± 0.3	− 0.02 ± 0.005	− 0.02 ± 0.003	− 0.02 ± 0.006	− 0.02 ± 0.002

Values are shown as means ± SEM. SR = strain rate.

*P <0.05 Control versus Diabetic in a given week. 2-tailed Student's t test. Control n = 8, Diabetic n = 8.

Table 3

Average long-axis (LAX) systolic and diastolic strain echocardiographic characteristics.

	Baseline		Week 1		Week 3		Week 6	
	Control	**Diabetic**	**Control**	**Diabetic**	**Control**	**Diabetic**	**Control**	**Diabetic**
LAX strain measurements in systole								
Longitudinal strain (%)	− 20.2 ± 0.9	− 21.4 ± 2.6	− 17.9 ± 0.6	− 16.7 ± 0.9	− 19.3 ± 1.0	− 18.5 ± 0.3	− 18.4 ± 1.2	− 18.7 ± 1.0
Longitudinal SR (1/s)	− 8.3 ± 0.6	− 7.5 ± 0.3	− 7.1 ± 0.3	− 6.7 ± 0.2	− 8.3 ± 0.3	− 6.8 ± 0.1*	− 8.5 ± 0.6	− 6.8 ± 0.4*
Longitudinal velocity (cm/s)	0.9 ± 0.06	0.9 ± 0.08	0.8 ± 0.04	0.9 ± 0.03	1.0 ± 0.05	0.9 ± 0.01	0.9 ± 0.05	0.9 ± 0.05
Longitudinal displacement (mm)	0.2 ± 0.02	0.2 ± 0.03	0.2 ± 0.01	0.2 ± 0.01	0.2 ± 0.02	0.2 ± 0.01	0.2 ± 0.02	0.2 ± 0.03
Radial strain (%)	28.8 ± 2.4	26.9 ± 3.0	27.8 ± 1.2	22.0 ± 1.1*	30.1 ± 2.0	24.7 ± 1.0*	27.7 ± 2.0	22.0 ± 0.6*
Radial SR (1/s)	8.6 ± 0.8	8.1 ± 0.4	8.1 ± 0.2	6.7 ± 0.2*	8.6 ± 0.4	6.9 ± 0.3*	7.6 ± 0.2	6.3 ± 0.3*
Radial velocity (cm/s)	1.5 ± 0.09	1.5 ± 0.1	1.3 ± 0.04	1.1 ± 0.04*	1.5 ± 0.08	1.2 ± 0.05*	1.4 ± 0.01	1.2 ± 0.05*
Radial displacement (mm)	0.5 ± 0.02	0.5 ± 0.04	0.5 ± 0.01	0.4 ± 0.01*	0.5 ± 0.02	0.5 ± 0.01	0.5 ± 0.01	0.4 ± 0.02
Long-axis strain measurements in diastole								
Longitudinal strain (%)	2.3 ± 0.4	2.4 ± 1.0	1.3 ± .02	1.3 ± 0.3	1.1 ± 0.2	1.6 ± 0.3	1.1 ± 0.2	0.9 ± 0.1
Longitudinal SR (1/s)	11.4 ± 0.7	11.5 ± 1.0	7.3 ± 0.2	7.9 ± 0.6	8.9 ± 0.6	9.8 ± 0.6	8.8 ± 0.6	10.0 ± 1.0
Longitudinal velocity (cm/s)	− 1.0 ± 0.08	− 1.1 ± 0.05	− 0.9 ± 0.01	− 1.0 ± 0.06	− 1.0 ± 0.05	− 0.9 ± 0.08	− 0.9 ± 0.06	− 1.0 ± 0.05
Longitudinal displacement (mm)	− 0.03 ± 0.01	− 0.04 ± 0.008	− 0.03 ± 0.004	− 0.04 ± 0.008	− 0.02 ± 0.005	− 0.04 ± 0.005	− 0.02 ± 0.006	− 0.04 ± 0.008
Radial strain (%)	− 2.8 ± 0.4	− 2.4 ± 0.5	− 1.6 ± 0.1	− 2.1 ± 0.3	− 1.6 ± 0.3	− 2.0 ± 0.3	− 2.1 ± 0.6	− 1.9 ± 0.4
Radial SR (1/s)	− 10.9 ± 1.1	− 10.5 ± 0.5	− 9.9 ± 0.6	− 9.1 ± 0.7	− 10.2 ± 0.6	− 10.2 ± 0.6	− 10.0 ± 0.4	− 10.3 ± 0.5
Radial velocity (cm/s)	− 2.0 ± 0.1	− 2.0 ± 0.1	− 1.5 ± 0.04	− 1.4 ± 0.08	− 1.6 ± 0.1	− 1.6 ± 0.1	− 1.6 ± 0.05	− 1.6 ± 0.09
Radial displacement (mm)	− 0.01 ± 0.002	− 0.008 ± 0.002	− 0.01 ± 0.001	− 0.01 ± 0.002	− 0.02 ± 0.003	− 0.01 ± 0.003	− 0.02 ± 0.004	− 0.02 ± 0.003

Values are shown as means ± SEM. SR = strain rate.

*P< 0.05 Control versus Diabetic in a given week. 2-tailed Student's t test. Control n = 8, Diabetic n = 8.